Chinese Physics C Vol. 50, No. 10 (2026) 103106

The role of triangle singularity in the $B^0 \to D^-\pi^+a_0(980)(\pi^0\eta)$ decay*

Wei Wang (王伟)[1] Dazhuang He (何大壮)[2] Xuan Luo (罗旋)[3†]

[1]School of Physics, Dalian University of Technology, Dalian 116024, China
[2]College of Physics and Electronic Engineering, Heze University, Heze 274015, China
[3]School of Physics and Optoelectronics Engineering, Anhui University, Hefei 230601, China

Abstract: The triangle singularity interpretation of the $a_1(1420)$ observed by the COMPASS Collaboration has been widely accepted. In this work, we investigate the triangle mechanism in the decay $B^0 \to D^-\pi^+a_0(980)(\pi^0\eta)$, where the $a_0(980)$ is treated as a dynamically generated state. The $\bar{K}^{*0}$-K^+-K^- triangle loop originates from the decay $B^0 \to D^-K^+\bar{K}^{*0}$, which has been observed by the Belle Collaboration, followed by the subsequent decay $\bar{K}^{*0} \to K^-\pi^+$. The triangle amplitude develops a pronounced peak around 1420 MeV, which is reflected in the invariant mass spectrum of the $\pi a_0(980)$ system. The differential decay width is calculated and exhibits a narrow peak around 980 MeV in the $\pi^0\eta$ invariant mass distribution. Furthermore, the invariant mass distribution of the $\pi^+\pi^0\eta$ system shows a clear peak around 1420 MeV, which further confirms the triangle singularity explanation of the $a_1(1420)$. We expect that the proposed B^0 decay mode could provide a potential platform for further exploring the triangle-singularity nature of the $a_1(1420)$ and could be tested in future experiments such as LHCb, BESIII, and Belle II.

Keywords: hadron states, triangle singularity, hadron decay

DOI: 10.1088/1674-1137/ae8005 **CSTR:** 32044.14.ChinesePhysicsC.50103106

I. INTRODUCTION

Over the past few decades, significant progress has been made in studies of the hadron spectrum, driven by the observation of numerous exotic states [1]. Although many of these exotic states can be interpreted as multiquark states or hadronic molecules, some observed structures may not correspond to poles of the S-matrix but may instead arise from kinematic singularities [2−4]. Among such kinematic effects, the triangle singularity (TS), first proposed by Landau in 1959 [5, 6], has attracted increasing interest. A triangle mechanism originates from the following sequential process: an initial particle A decays into two internal particles, labeled 1 and 2, which move back-to-back in the rest frame of A. Particle 2 subsequently decays into an internal particle 3 and an external particle B, with particle 3 moving in the same direction as particle 1. The two internal particles 1 and 3 then undergo rescattering and form an external particle C. According to the Coleman-Norton theorem [7], the emergence of a TS depends on whether the above processes can be interpreted as a classical scattering process and whether all three internal particles can simultaneously go on shell and become collinear in the rest frame of the decaying particle [5]. In reality, the internal particles have finite widths, which smear the singular behavior and transform the TS into a finite peak that can be observed experimentally.

Phenomenological studies have successfully applied the TS mechanism to explain a variety of long-standing puzzles in hadron physics. The anomalously large isospin violation observed in the decay $J/\psi \to \gamma\eta(1405/1475) \to \gamma\pi^0 f_0(980) \to \gamma 3\pi$, reported by the BESIII Collaboration [8], was interpreted in terms of the TS in Ref. [9]. This mechanism has contributed to a better understanding of the nature of the two nearby states $\eta(1405)$ and $\eta(1475)$, as well as the mixing between the $a_0(980)$ and $f_0(980)$ resonances, which has been further investigated in a series of subsequent works [10−14]. Meanwhile, the triangle mechanism has also been employed to interpret the properties of heavy exotic hadronic states, such as the $Y(4260)$, $Z_c(3900)$, $Z_b(10610)$, and $Z_b(10650)$, in various processes [15−23]. A milestone in the development of the triangle mechanism was achieved in Ref.

Received 29 January 2026; Accepted 22 June 2026; Accepted manuscript online 23 June 2026

* Dazhuang He is supported by the Heze University doctoral fund project (010008002039037). Xuan Luo is supported by the National Natural Science Foundation of China (12205002)

† E-mail: xuanluo@ahu.edu.cn

[24], where a detailed analysis of the singularities in a triangle loop integral was presented and a compact formula was derived for evaluating the TS on the physical boundary. This formalism was successfully applied to the decay $\Lambda_b \to J/\psi K^- p$ through a Λ^*-charmonium-proton triangle loop. Thereafter, the triangle mechanism involving an $f_0(980)$ or $a_0(980)$ final state was further explored in a variety of processes [25−31]. In Ref. [26], the authors identified two nonresonant peaks associated with the TS at approximately 2850 and 3000 MeV in the invariant mass distributions of the πD_{s0} and πD_{s1} systems, respectively. That work also demonstrated the relation between the structure of the triangle amplitude and the finite widths of the internal particles in the loop. A comprehensive review of threshold cusps and various TS structures in hadronic reactions can be found in Ref. [32], where their roles in phenomena related to exotic hadron candidates are systematically summarized.

The triangle mechanism has been extensively discussed in a wide range of hadronic decays involving charmonium [33−39], the Λ baryon family [40−46], and the D-meson sector [47−50]. In addition, decays of the B-meson family provide a promising platform for probing this mechanism, such as $B^- \to D^{*0}\pi^-\pi^+\pi^-(\pi^0\eta)$ [26], $B^- \to K^-\pi^0 X(3872)$ [51], $B^- \to K^- X(3872)$ with $X(3872) \to \pi^0\pi^+\pi^-$ [52], $B^- \to K^-\pi^- D^+_{s0/s1}$ [53], $B^+ \to J/\psi\phi K^+$ [54], $B^+ \to J/\psi\pi^+\pi^0 K^0$ and $B^+ \to J/\psi\pi^+\pi^- K^+$ [55], $B^+ \to D^- D^+_s \pi^+$ and $B^0 \to \bar{D}^0 D^+_s \pi^-$ [56], $B^0 \to J/\psi K^0 f_0(980)(a_0(980))$ [31], $\bar{B}^0 \to \chi_{c1} K^-\pi^+$ [57], $B \to (J/\psi\pi^+\pi^-)K\pi$ [58], $\bar{B}^0_s \to J/\psi\pi^0 f_0(980)$ [29], and $B_c \to B_s\pi\pi$ [59]. Beyond hadronic decays, the triangle mechanism has also been explored in a variety of other processes, including semileptonic τ-lepton decays [60−62], photon-proton collisions [63, 64], electron-positron annihilation [65, 66], and proton-proton collisions [67, 68]. Furthermore, an interesting study [69] discussed the structure of TS involving new-physics particles at high-energy colliders. In addition, numerous other investigations have been devoted to the triangle mechanism and its phenomenological implications [70−81].

In particular, the TS explanation for the observation of the $a_1(1420)$ reported by the COMPASS Collaboration [82, 83] has been widely accepted. In this mechanism, the $a_1(1260)$ first decays into $K^*\bar{K}$, with $K^* \to \pi K$, after which the $K\bar{K}$ pair fuses to form the $f_0(980)$, giving the observed $\pi f_0(980)$ decay mode. In addition, it has also been studied in various processes [28, 29, 37, 40, 60, 84]. Based on previous studies, in this work we explore the physical effects of the TS and identify its contribution to the $B^0 \to D^-\pi^+ a_0(980)$ decay. The observation of the weak decay $B^0 \to D^- K^+ \bar{K}^{*0}$ by the Belle Collaboration [85], together with the cascade decay $\bar{K}^{*0} \to K^-\pi^+$, allows the construction of a $\bar{K}^{*0}$-K-K triangle loop. As we will show, the invariant mass of the $\bar{K}^{*0}K^+$ system in the B^0 decay allows the production of the $a_0(980)$ in the region where the TS condition is satisfied. This leads to a pronounced peak structure in the $\pi^+ a_0(980)$ invariant mass spectrum around 1420 MeV. In the above calculation, the triangle amplitude is evaluated following the analytical formulations developed in Refs. [24, 32]. Furthermore, within the chiral unitary approach, the $a_0(980)$ can be regarded as a dynamically generated state arising from meson-meson interactions [86−88]. An enhancement around 980 MeV is expected to be reproduced in the $\pi^0\eta$ invariant mass distribution. Consequently, the $B^0 \to D^-\pi^+ a_0(980)(\pi^0\eta)$ decay provides a potential platform to investigate both the TS structure associated with the $\bar{K}^{*0}$-K-K triangle loop and the nature of the $a_0(980)$ resonance.

The paper is organized as follows. In Sec. II, we present the theoretical formalism and detail the kinematic conditions for the $\bar{K}^{*0}$-K-K triangle loop considered here. In Sec. III, the weak decay mechanism for $B^0 \to D^- K^+ \bar{K}^{*0}$ is described, and the effective coupling strength is extracted from current experimental measurements. In Sec. IV, we formulate the $B^0 \to D^-\pi^+ a_0(980)$ decay by incorporating the triangle mechanism and provide the details of the derivation. The $a_0(980)$ is further treated as a dynamically generated state, and the sequential process $B^0 \to D^-\pi^+ a_0(980)$ with $a_0(980) \to \pi^0\eta$ is analyzed. In Sec. V, we present the numerical results for these processes. The peaks around 1420 and 980 MeV are reproduced in the invariant mass distributions of the πa_0 and $\pi^0\eta$ systems, respectively. Finally, a brief summary is provided in Sec. VI.

II. FORMALISM

In this section, we show that a peak structure around 1420 MeV, induced by the TS, can be generated in the $B^0 \to D^-\pi^+ a_0(980)$ decay. The Feynman diagram is shown in the left panel of Fig. 1. In this process, the B^0 first decays into $D^-\bar{K}^{*0}K^+$, after which the $\bar{K}^{*0}$ decays into K^- and π^+. The K^+ and K^- move in the same direction, with the K^- moving faster than the K^+, allowing the K^+K^- pair to fuse into the $a_0(980)$. The channel $B^0 \to D^-\bar{K}^0 K^{*+}$ has not yet been observed experimentally. Therefore, the contribution of the K^{*+}-$\bar{K}^0$-K^0 triangle loop from the $B^0 \to D^-\bar{K}^0 K^{*+}$ decay is not considered in the present work. Furthermore, the $a_0(980)$ can be interpreted as a dynamically generated state with isospin $I=1$, arising from the coupled channels $\pi^0\eta$, K^+K^-, and $K^0\bar{K}^0$ within the chiral unitary approach [87, 88]. The decay of $a_0(980)$ is shown in the right panel of Fig. 1.

The TS occurs when the kinematic variables of the internal particles satisfy the following condition

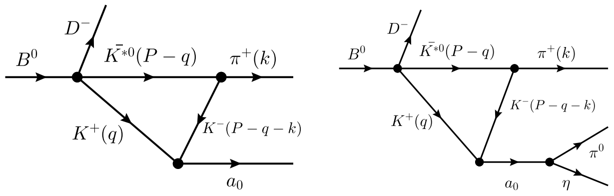

Fig. 1. The Feynman diagrams for the $B^0 \to D^-\pi^+a_0(980)$ and $B^0 \to D^-\pi^+a_0(980), a_0(980) \to \pi^0\eta$ processes involving a $\bar{K}^*$-K-$\bar{K}$ triangle loop are shown in the left and right panels, respectively.

$$\lim_{\epsilon\to 0}\left(q_+^{\rm on} - q_-^{\rm a}\right) = 0,$$
$$q_+^{\rm on} = \frac{\lambda^{\frac{1}{2}}\left(m_{\rm inv}^2(\pi a_0), m_K^2, m_{\bar{K}^{*0}}^2\right)}{2m_{\rm inv}(\pi a_0)} + {\rm i}\epsilon, \tag{1}$$

where $q_+^{\rm on}$ denotes the on-shell three-momentum of K^+ in the center-of-mass frame (COM) of the $\bar{K}^{*0}K^+$ system. The quantity $m_{\rm inv}(\pi a_0)$ is the invariant mass of the $\bar{K}^{*0}K^+$ system, and $\lambda(x,y,z) = x^2+y^2+z^2-2xy-2yz-2xz$ is the Källén function. Meanwhile, $q_-^{\rm a}$ is given by

$$q_-^{\rm a} = \gamma(\nu E_{K^-}^* - p_{K^-}^*) - {\rm i}\epsilon, \tag{2}$$

with the definitions

$$\nu = \frac{k}{E_{a_0}}, \qquad \gamma = \frac{1}{\sqrt{1-\nu^2}} = \frac{E_{a_0}}{m_{a_0}},$$
$$E_{K^-}^* = \frac{m_{a_0}}{2}, \qquad p_{K^-}^* = \frac{\lambda^{\frac{1}{2}}(m_{a_0}^2, m_K^2, m_K^2)}{2m_{a_0}}, \tag{3}$$

where $E_{K^-}^*$ and $p_{K^-}^*$ are the energy and momentum of the K^- meson in the rest frame of a_0. ν and γ denote the velocity of the K^+K^- system and the Lorentz boost factor, respectively. Eq. (1) implies that all three particles in the loop are on shell and that K^+ in the rest frame of $a_0(980)$ and $a_0(980)$ in the COM frame of $\pi a_0(980)$ move in the same direction. The formation of $a_0(980)$ through K^+K^- fusion further requires that the momentum of K^+ in the COM frame of πa_0 be smaller than that of K^- in the rest frame of $\bar{K}^{*0}$. Equivalently, Eq. (1) can be understood as the condition that q_-^a and $q_+^{\rm on}$ represent the singularities of the triangle loop function in the upper and lower halves of the complex-q plane, respectively. The integration contour of the loop function in Eq. (21) is then pinched between q_-^a and $q_+^{\rm on}$ at the same point on the real axis. Consequently, solving Eq. (1) yields a TS around 1420 MeV in the $m_{\rm inv}(\pi a_0)$ invariant mass distribution. When the finite width of the $\bar{K}^{*0}$ is taken into account by replacing $m_{\bar{K}^{*0}} \to m_{\bar{K}^{*0}} - {\rm i}\Gamma_{\bar{K}^{*0}}/2$ with $\Gamma_{\bar{K}^{*0}} = 47$ MeV, the TS moves into the complex plane, yielding 1420.7−i28.0 MeV.

III. THE $B^0 \to D^-K^+\bar{K}^{*0}$ DECAY

To evaluate the amplitude shown in Fig. 1, the effective coupling strength of the $B^0 \to D^-K^+\bar{K}^{*0}$ vertex is required. The B^0 meson can decay into the $D^-K^+\bar{K}^{*0}$ final state through the weak decay of the b quark, as illustrated in Fig. 2. At the quark level, the b quark undergoes a weak transition into a c quark through the emission of a W boson and hadronizes into the D^- meson. The emitted W boson subsequently decays into a $u\bar{d}$ pair, which combines with an additional $q\bar{q}$ pair from the vacuum to form the $\bar{K}^{*0}K^+$ final state.

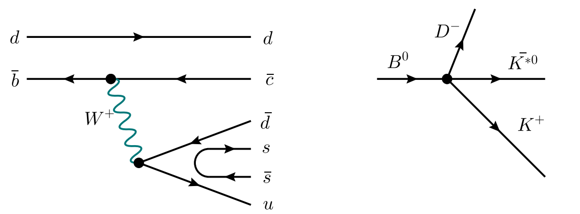

Fig. 2. (color online) The quark-level and hadron-level Feynman diagrams for the decay $B^0 \to D^-K^+\bar{K}^{*0}$ are shown in the left and right panels, respectively.

The interaction of the effective vertex in Fig. 2 can be constructed using the P-wave interaction. Following the convention adopted in Refs. [28, 53], we write

$$-{\rm i}t_{B\to DK\bar{K}^{*0}} = -{\rm i}C\vec{\epsilon}_{\bar{K}^{*0}} \cdot \vec{p}_D, \tag{4}$$

where $\vec{\epsilon}_{\bar{K}^{*0}}$ and $\vec{p}_D$ are the polarization vector of the $\bar{K}^{*0}$ and the momentum of the D^-, respectively. Below, we present the details of the calculation of the vertex coupling strength C. By solving Eq. (1), a TS around 1420 MeV is obtained. The three-momentum of the $\bar{K}^{*0}$ in the πa_0 rest frame is approximately 135.66 MeV, which is smaller than the $\bar{K}^{*0}$ mass of 895.81 MeV. Therefore, the time component ϵ^0 of the $\bar{K}^{*0}$ polarization vector can be safely neglected. We take the polarization sum for the $\bar{K}^{*0}$ as

$$\sum_{\mu,\nu}\epsilon_{\bar{K}^{*0}\mu}\epsilon_{\bar{K}^{*0}\nu} \sim \sum_{i,j}\epsilon_{\bar{K}^{*0}i}\epsilon_{\bar{K}^{*0}j} = \delta_{ij};$$
$$\mu = i,\ \mu = j; \qquad i,j = 1,2,3. \tag{5}$$

The decay width for the process $B \to DK\bar{K}^{*0}$ is given by

$$\Gamma_{B\to DK\bar{K}^{*0}} = \int {\rm d}m_{\rm inv}(\bar{K}^{*0}K^+)$$
$$\times \frac{1}{(2\pi)^3}\frac{|\vec{p}_D||\vec{p}^{\,\prime}_{\bar{K}^{*0}}|}{4m_B^2}\sum_{\rm pol}|t_{B\to DK\bar{K}^{*0}}|^2, \tag{6}$$

where $m_{\rm inv}(\bar{K}^{*0}K^+)$ is the invariant mass of the $\bar{K}^{*0}K^+$ system. Here, $\vec{p}\,'_{\bar{K}^{*0}}$ and $\vec{p}_D$ denote the three-momenta of the $\bar{K}^{*0}$ in the $\bar{K}^{*0}K^+$ COM frame and of the D^- in the B^0 rest frame, respectively. They are given by

$$|\vec{p}_D| = \frac{\lambda^{\frac{1}{2}}\left(m_B^2,\, m_{\rm inv}^2(\bar{K}^{*0}K^+),\, m_D^2\right)}{2m_B},$$
$$|\vec{p}\,'_{\bar{K}^{*0}}| = \frac{\lambda^{\frac{1}{2}}\left(m_{\rm inv}^2(\bar{K}^{*0}K^+),\, m_K^2,\, m_{\bar{K}^{*0}}^2\right)}{2m_{\rm inv}(\bar{K}^{*0}K^+)}. \quad (7)$$

After squaring the amplitude $t_{B\to DK\bar{K}^{*0}}$ and applying the polarization sum in Eq. (5), we obtain

$$\sum_{\rm pol}|t_{B\to DK\bar{K}^{*0}}|^2 = C^2|\vec{p}\,'_D|^2, \quad (8)$$

where $\vec{p}\,'_D$ is the three-momentum of the D^- in the COM frame of the $\bar{K}^{*0}K^+$ system.

$$|\vec{p}\,'_D| = \frac{\lambda^{\frac{1}{2}}\left(m_B^2,\, m_{\rm inv}^2(\bar{K}^{*0}K^+),\, m_D^2\right)}{2m_{\rm inv}(\bar{K}^{*0}K^+)}. \quad (9)$$

From recent measurements [1, 85], the partial decay branching fraction is given by ${\rm Br}(B^0\to D^-K^+\bar{K}^{*0})$ =$(7.7\pm 0.6)\times10^{-4}$. Combining Eq. (6) with Eq. (8), we obtain

$$\frac{C^2}{\Gamma_{B^0}} = \frac{{\rm Br}\left(B^0\to D^-K^+\bar{K}^{*0}\right)}{\displaystyle\int {\rm d}m_{\rm inv}(\bar{K}^{*0}K^+)\frac{1}{(2\pi)^3}\frac{|\vec{p}_D||\vec{p}\,'_{\bar{K}^{*0}}|}{4m_B^2}|\vec{p}\,'_D|^2}. \quad (10)$$

IV. THE $B^0\to D^-\pi^+a_0(980)$ DECAY

The amplitude for the $B^0\to D^-\pi^+a_0(980)$ decay (left panel of Fig. 1) can be written as

$$-{\rm i}t_{B\to D\pi a_0} = {\rm i}\sum_{\rm pol}\int\frac{{\rm d}^4q}{(2\pi)^4}\frac{{\rm i}t_{B\to DK\bar{K}^{*0}}}{q^2-m_K^2+{\rm i}\epsilon}$$
$$\times\frac{{\rm i}t_{\bar{K}^{*0}K^-\pi^+}}{(P-q)^2-m_{\bar{K}^{*0}}^2+{\rm i}\epsilon}\frac{{\rm i}t_{K^+K^-a_0}}{(P-q-k)^2-m_K^2+{\rm i}\epsilon}, \quad (11)$$

in the COM frame of the πa_0 system, where the π^+ originates from the $\bar{K}^{*0}$ decay. In Eq. (11), the amplitude $t_{B\to DK\bar{K}^{*0}}$ was calculated in the previous section (Sec. III). The amplitude $t_{\bar{K}^{*0}K^-\pi^+}$ can be calculated using the chiral-invariant Lagrangian with local hidden symmetry [89, 90] and is given by

$$\mathcal{L}_{\rm VPP} = -{\rm i}g\langle V^\mu[P,\partial_\mu P]\rangle, \quad (12)$$

where bracket $\langle\cdots\rangle$ denotes the $SU(3)$ trace, and the coupling constant is given by $g=m_V/2f_\pi$, with $m_V=800$ MeV and $f_\pi=93$ MeV, within the local hidden gauge formalism. P and V^μ represent the pseudoscalar and vector meson octets, respectively, which are given by

$$P = \begin{pmatrix} \frac{\pi^0}{\sqrt{2}}+\frac{\eta_8}{\sqrt{6}} & \pi^+ & K^+ \\ \pi^- & -\frac{\pi^0}{\sqrt{2}}+\frac{\eta_8}{\sqrt{6}} & K^0 \\ K^- & \bar{K}^0 & -\frac{2}{\sqrt{6}}\eta_8 \end{pmatrix},$$
$$V = \begin{pmatrix} \frac{\rho^0}{\sqrt{2}}+\frac{\omega}{\sqrt{2}} & \rho^+ & K^{*+} \\ \rho^- & -\frac{\rho^0}{\sqrt{2}}+\frac{\omega}{\sqrt{2}} & K^{*0} \\ K^{*-} & \bar{K}^{*0} & \phi \end{pmatrix}. \quad (13)$$

Then, the amplitude for the decay $\bar{K}^{*0}\to K^-\pi^+$ can be written as

$$-{\rm i}t_{\bar{K}^{*0}K^-\pi^+} = -{\rm i}g\vec{\epsilon}_{\bar{K}^{*0}}\cdot(\vec{p}\,'_{\pi^+}-\vec{p}\,'_{K^-}). \quad (14)$$

As in Eq. (8), we neglect the time component of the polarization vector in Eq. (14) and employ the polarization sum given in Eq. (5). Here, $\vec{p}\,'_{\pi^+}$ and $\vec{p}\,'_{K^-}$ denote the three-momenta of the π^+ and K^- in the COM frame of the πa_0 system, respectively. The momentum $\vec{p}\,'_{\pi^+}$ is given by

$$|\vec{p}\,'_{\pi^+}| = |\vec{k}| = \frac{\lambda^{\frac{1}{2}}\left(m_{\rm inv}^2(\pi a_0),\, m_\pi^2,\, m_{a_0}^2\right)}{2m_{\rm inv}(\pi a_0)}. \quad (15)$$

As discussed in Sec. II, the $a_0(980)$ is considered to be a dynamically generated state. The amplitude $t_{K^+K^-a_0}$ can be written directly as

$$t_{K^+K^-a_0} = g_{K^+K^-a_0}. \quad (16)$$

Above, we set $g_{K^+K^-a_0}=3875$ MeV [87]. Thus, the amplitude expression in Eq. (11) can be simplified to

$$t_{B\to D\pi a_0(980)} = {\rm i}g_{K^+K^-a_0}gC\sum_{\rm pol}\int\frac{{\rm d}^4q}{(2\pi)^4}$$
$$\times\frac{\vec{\epsilon}_{\bar{K}^{*0}}\cdot\vec{p}\,'_D}{q^2-m_K^2+{\rm i}\epsilon}\frac{\vec{\epsilon}_{\bar{K}^{*0}}\cdot(\vec{p}\,'_{\pi^+}-\vec{p}\,'_{K^-})}{(P-q)^2-m_{\bar{K}^{*0}}^2+{\rm i}\epsilon}$$
$$\times\frac{1}{(P-q-k)^2-m_K^2+{\rm i}\epsilon}, \quad (17)$$

where $\vec{p}\,'_{\pi^+}$ is given in Eq. (15). The quantity $\vec{p}\,'_D$ is the momentum of the D^- in the COM frame of πa_0, which originates from the B^0 decay.

$$|\vec{p}_D'| = \frac{\lambda^{\frac{1}{2}}\left(m_B^2,\, m_{\rm inv}^2(\pi a_0),\, m_D^2\right)}{2m_{\rm inv}(\pi a_0)}. \tag{18}$$

Equation (5) is used to perform the polarization sum in Eq. (17), yielding

$$\begin{aligned} t_{B\to D\pi a_0(980)} =& \mathrm{i} g_{K^+K^-a_0} g C \int \frac{\mathrm{d}^4 q}{(2\pi)^4} \\ &\times \frac{1}{q^2-m_K^2+\mathrm{i}\epsilon} \frac{\vec{p}_D'\cdot(2\vec{k}+\vec{q})}{(P-q)^2-m_{\bar{K}^{*0}}^2+\mathrm{i}\epsilon} \\ &\times \frac{1}{(P-q-k)^2-m_K^2+\mathrm{i}\epsilon}, \end{aligned} \tag{19}$$

where $\vec{p}_{\pi^+}' - \vec{p}_{K^-}' = \vec{k}-(-\vec{k}-\vec{q}) = 2\vec{k}+\vec{q}$. P is the momentum of the πa_0 system in its rest frame.

$$P = (m_{\rm inv}(\pi a_0),\, 0,\, 0,\, 0). \tag{20}$$

The quantity t_T is defined to describe the loop integral in Eq. (19) as

$$\begin{aligned} t_T =& \mathrm{i}\int \frac{\mathrm{d}^4 q}{(2\pi)^4}\, \vec{p}_D'\cdot(2\vec{k}+\vec{q}) \frac{1}{q^2-m_K^2+\mathrm{i}\epsilon} \\ &\times \frac{1}{(P-q)^2-m_{\bar{K}^{*0}}^2+\mathrm{i}\epsilon} \frac{1}{(P-q-k)^2-m_K^2+\mathrm{i}\epsilon}. \end{aligned} \tag{21}$$

Following Refs. [24, 32], the negative-energy part of the $\bar{K}^{*0}$ propagator in t_T can be neglected. The integration over dq^0 in t_T is performed by applying the residue theorem and using the following formula

$$\int \mathrm{d}^3 q\, \vec{q}_i\, f(\vec{q},\vec{k}) = \vec{k}_i \int \mathrm{d}^3 q \frac{\vec{q}\cdot\vec{k}}{|\vec{k}|^2} f(\vec{q},\vec{k}). \tag{22}$$

Now, the triangle loop amplitude t_T reduces to

$$\begin{aligned} t_T =& \vec{p}_D'\cdot\vec{k}\int \frac{\mathrm{d}^3 q}{(2\pi)^3}\left(2+\frac{\vec{q}\cdot\vec{k}}{|\vec{k}|^2}\right) \\ &\times \frac{1}{8\omega_{K^+}(\vec{q})\,\omega_{K^-}(\vec{q}+\vec{k})\,\omega_{K^*}(\vec{q})} \\ &\times \frac{1}{k^0-\omega_{K^-}(\vec{q}+\vec{k})-\omega_{K^*}(\vec{q})+\mathrm{i}\epsilon} \\ &\times \frac{1}{P^0-\omega_{K^*}(\vec{q})-\omega_{K^+}(\vec{q})+\mathrm{i}\epsilon} \\ &\times \frac{1}{P^0-\omega_{K^+}(\vec{q})-\omega_{K^-}(\vec{q}+\vec{k})-k^0+\mathrm{i}\epsilon} \\ &\times \frac{1}{P^0+\omega_{K^+}(\vec{q})+\omega_{K^-}(\vec{q}+\vec{k})-k^0+\mathrm{i}\epsilon} \\ &\times \Big\{2P^0\omega_{K^+}(\vec{q})+2k^0\omega_{K^-}(\vec{q}+\vec{k}) \\ &-2\left[\omega_{K^+}(\vec{q})+\omega_{K^-}(\vec{q}+\vec{k})\right] \\ &\times\left[\omega_{K^+}(\vec{q})+\omega_{K^-}(\vec{q}+\vec{k})+\omega_{K^*}(\vec{q})\right]\Big\}, \\ =& \vec{p}_D'\cdot\vec{k}\times\tilde{t}_T, \end{aligned} \tag{23}$$

where $\omega_{K^+}(\vec{q}) = \sqrt{m_K^2+\vec{q}^2}$, $\omega_{K^{*0}}(\vec{q}) = \sqrt{m_{\bar{K}^{*0}}^2+\vec{q}^2}$, and $\omega_{K^-}(\vec{q}+\vec{k}) = \sqrt{m_K^2+(\vec{k}+\vec{q})^2}$. From Eq. (20), $P^0 = m_{\rm inv}(\pi a_0)$ is the invariant mass of the πa_0 system. Although the integral in Eq. (23) is convergent, the chiral unitary approach naturally provides an upper limit $q_{\rm max}$ [10, 13]. In this work, we use $q_{\rm max} = 600$ MeV for $a_0(980)$ production [86, 91]. To reproduce the peak observed in experiments, the finite width of the $\bar{K}^{*0}$ in the triangle loop must be taken into account. This is implemented by replacing ω_{K^*} with $\omega_{K^*}-\mathrm{i}\Gamma_{\bar{K}^{*0}}/2$ in the denominator of Eq. (23).

Finally, the differential decay width for the three-body final state $B^0 \to D^-\pi^+a_0(980)$ is given by

$$\begin{aligned} \frac{\mathrm{d}\Gamma'}{\mathrm{d}m_{\rm inv}(\pi a_0)} =& \frac{2}{3}\frac{1}{(2\pi)^3}\frac{C^2 g_{K^+K^-a_0}^2 g^2}{8m_B^2} \\ &\times|\vec{p}_D||\vec{p}_D'|^2|\vec{k}|^3|\tilde{t}_T|^2. \end{aligned} \tag{24}$$

The factor $2/3$ in Eq. (24) originates from the angular phase-space integration of the integrand in $\vec{p}_D'\cdot\vec{k} = |\vec{p}_D'||\vec{k}|\cos\theta$. Here, $\vec{p}_D$ denotes the momentum of the D^- in the B^0 rest frame.

$$|\vec{p}_D| = \frac{\lambda^{\frac{1}{2}}\left(m_B^2, M_{D^-}^2, m_{\rm inv}^2(\pi a_0)\right)}{2m_B}. \tag{25}$$

In addition, we further explore the possibility of observing the $a_0(980)$ through the $\pi^0\eta$ final state. Following Ref. [53], the $a_0(980)$ appears as an unstable resonance in the B^0 decay and subsequently decays into $\pi^0\eta$. Therefore, we consider the corresponding four-body decay, as illustrated in the right panel of Fig. 1. In this process, the $a_0(980)$ resonance can be treated as an intermediate particle, allowing us to include an additional differential distribution with respect to the $\pi\eta$ invariant mass in Eq. 24. The differential decay width for $B^0 \to D^-\pi^+\pi^0\eta$ is then given by

$$\begin{aligned} \frac{\mathrm{d}\Gamma'}{\mathrm{d}m_{\rm inv}(\pi a_0)} =& \frac{1}{3}\frac{1}{(2\pi)^3}\frac{g^2C^2}{4m_B^2}\int \mathrm{d}m_{\rm inv}^2(\pi\eta) \\ &\times\left(-\frac{1}{\pi}\mathrm{Im}D\right) g_{K^-K^+a_0}^2|\vec{p}_D||\vec{p}_D'|^2|\vec{k}|^3|\tilde{t}_T|^2, \end{aligned} \tag{26}$$

with

$$D = \frac{1}{m_{\rm inv}^2(\pi\eta) - m_{a_0}^2 + {\rm i} m_{a_0}\Gamma_{a_0}}, \tag{27}$$

where $m_{\rm inv}(\pi\eta)$ is the invariant mass of the $\pi\eta$ system produced in the $a_0(980)$ decay, and m_{a_0} is the mass of $a_0(980)$. Eq. (26) reduces to Eq. (24) in the limit $\Gamma_{a_0} \to 0$, where ${\rm i\,Im}\,D \to -{\rm i}\pi\delta\left(m_{\rm inv}^2(\pi\eta) - m_{a_0}^2\right)$. Thus, Eq. (26) simplifies to

$$\frac{{\rm d}\Gamma'}{{\rm d}m_{\rm inv}(\pi a_0)} = \frac{1}{3\pi}\frac{1}{(2\pi)^3}\frac{g^2C^2}{4m_B^2}\int {\rm d}m_{\rm inv}^2(\pi\eta) \times \frac{g_{K^-K^+a_0}^2|\vec{p}_D||\vec{p}_D^{\,\prime}|^2|\vec{k}|^3|\tilde{t}_T|^2 m_{a_0}\Gamma_{a_0}}{\left[m_{\rm inv}^2(\pi\eta) - m_{a_0}^2\right]^2 + (m_{a_0}\Gamma_{a_0})^2}. \tag{28}$$

The decay width Γ_{a_0} is calculated by considering the $a_0 \to \pi^0\eta$ decay

$$\Gamma_{a_0} = \frac{1}{8\pi}\frac{g_{a_0\pi\eta}^2}{m_{\rm inv}^2(\pi\eta)}|\vec{q}_\eta|, \tag{29}$$

where $|\vec{q}_\eta|$ denotes the magnitude of the η momentum in the rest frame of $a_0(980)$ and is given by

$$|\vec{q}_\eta| = \frac{\lambda^{\frac{1}{2}}\left(m_{\rm inv}^2(\pi\eta), m_\pi^2, m_\eta^2\right)}{2m_{\rm inv}(\pi\eta)}. \tag{30}$$

By substituting Eq. (29) into Eq. (28), we obtain

$$\frac{{\rm d}\Gamma'}{{\rm d}m_{\rm inv}(\pi a_0)} = \frac{1}{(2\pi)^5}\frac{g^2C^2}{24m_B^2}\int {\rm d}m_{\rm inv}^2(\pi\eta) \times |\vec{p}_D||\vec{p}_D^{\,\prime}|^2|\vec{k}|^3|\tilde{t}_T|^2\frac{|\vec{q}_\eta|}{m_{\rm inv}^2(\pi\eta)} \times \frac{m_{a_0}g_{K^-K^+a_0}^2 g_{a_0\pi\eta}^2}{\left[m_{\rm inv}^2(\pi\eta) - m_{a_0}^2\right]^2 + (m_{a_0}\Gamma_{a_0})^2}. \tag{31}$$

Meanwhile, the amplitude for the $K^+K^- \to \pi\eta$ process mediated by exchange of the $a_0(980)$ resonance can be written as

$$\frac{g_{K^-K^+a_0}^2 g_{a_0\pi\eta}^2}{\left[m_{\rm inv}^2(\pi\eta) - m_{a_0}^2\right]^2 + (m_{a_0}\Gamma_{a_0})^2} = |t_{K^+K^-\to\pi\eta}|^2. \tag{32}$$

In contrast, when the $a_0(980)$ is treated as a dynamically generated state, the amplitude $t_{K^+K^-\to\pi\eta}$ can be calculated by solving the Bethe–Salpeter (BS) equation within the chiral unitary approach. The BS equation is given by

$$T = [1 - VG]^{-1}V. \tag{33}$$

Here, G denotes the loop function for two meson propagators [86].

$$G(s) = {\rm i}\int \frac{{\rm d}^4q}{(2\pi)^4}\frac{1}{(P-q)^2 - m_1^2 + {\rm i}\epsilon}\frac{1}{q^2 - m_2^2 + {\rm i}\epsilon}, \tag{34}$$

and is regularized by a cutoff $q_{\rm max}$ as

$$G(s) = \frac{1}{16\pi^2 s}\left\{\sigma\left(\arctan\frac{s+\Delta}{\sigma\lambda_1} + \arctan\frac{s-\Delta}{\sigma\lambda_2}\right) - \left[(s+\Delta)\ln\frac{(1+\lambda_1)q_{\rm max}}{m_1} + (s-\Delta)\ln\frac{(1+\lambda_2)q_{\rm max}}{m_2}\right]\right\},$$

with

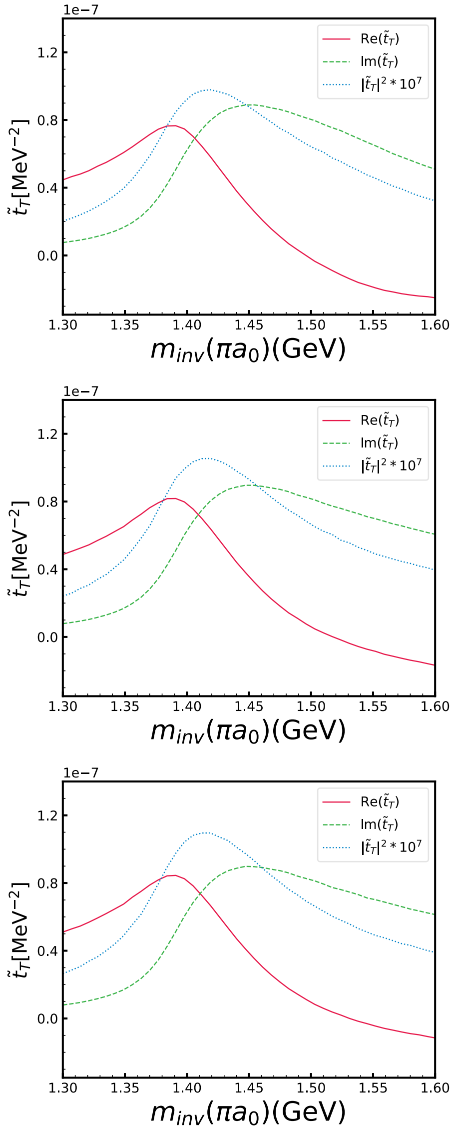

Fig. 3. (color online) The $\bar{K}^{*0}K^+K^-$ triangle amplitudes $\tilde{t}_T$ for $q_{\rm max} = 600, 800, 1000$ MeV are shown from top to bottom, respectively. We set $m_{a_0} = 980$ MeV, and $\tilde{t}_T^2$ is multiplied by 10^7.

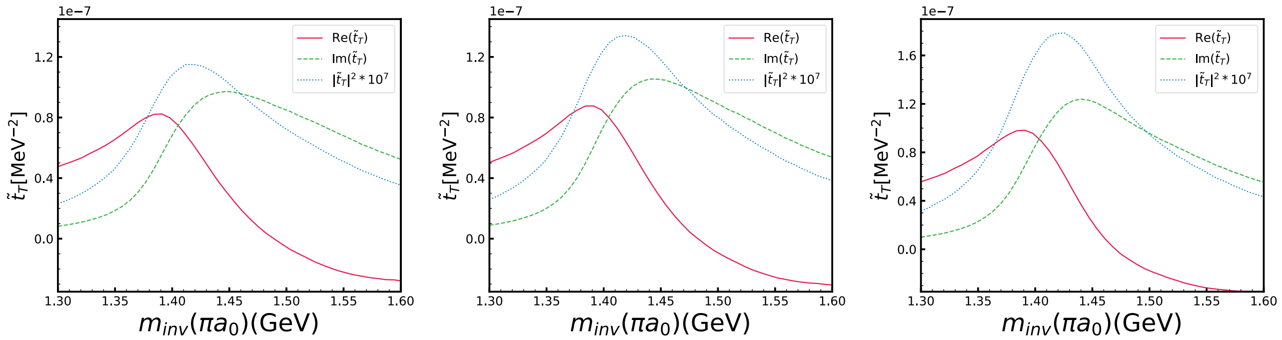

Fig. 4. (color online) As in Fig. 3, the triangle amplitudes for $m_{a_0} = 983$, 985, and 987 MeV with $q_{\max} = 600$ MeV are shown.

$$\sigma = \left[-(s-(m_1+m_2)^2)(s-(m_1-m_2)^2)\right]^{1/2},$$

$$\Delta = m_1^2 - m_2^2,\ \ \lambda_1 = \sqrt{1+\frac{m_1^2}{q_{\max}^2}},\ \ \lambda_2 = \sqrt{1+\frac{m_2^2}{q_{\max}^2}}\ .$$

A value of $q_{\max} = 600$ MeV is used to reproduce the $a_0(980)$ around 980 MeV. The meson-meson interaction potentials for the case $I = 1$ are given as follows [86]:

$$\begin{aligned} V_{K^+K^-\to K^+K^-} &= -\frac{1}{2f_\pi^2}s, \quad V_{K^+K^-\to K^0\bar{K}^0} = -\frac{1}{4f_\pi^2}s, \\ V_{K^+K^-\to\pi^0\eta} &= \frac{-\sqrt{3}}{12f_\pi^2}\left(3s-\frac{8}{3}m_K^2-\frac{1}{3}m_\pi^2-m_\eta^2\right), \\ V_{K^0\bar{K}^0\to K^0\bar{K}^0} &= -\frac{1}{2f_\pi^2}s, \quad V_{\pi^0\eta\to\pi^0\eta} = -\frac{m_\pi^2}{3f_\pi^2}, \\ V_{K^0\bar{K}^0\to\pi^0\eta} &= -V_{K^+K^-\to\pi^0\eta}. \end{aligned} \tag{35}$$

Finally, the double-differential distribution of the B^0 decay can be written as

$$\frac{1}{\Gamma_{B^0}}\frac{\mathrm{d}^2\Gamma'}{\mathrm{d}m_{\rm inv}(\pi a_0)\mathrm{d}m_{\rm inv}(\pi\eta)} = \frac{C^2}{\Gamma_{B^0}}\frac{g^2}{(2\pi)^5} \times \frac{|\vec{p}_D||\vec{p}_D'|^2|\vec{k}|^3|\vec{q}_\eta|}{12m_B^2}|\tilde{t}_T\times t_{K^+K^-\to\pi\eta}|^2. \tag{36}$$

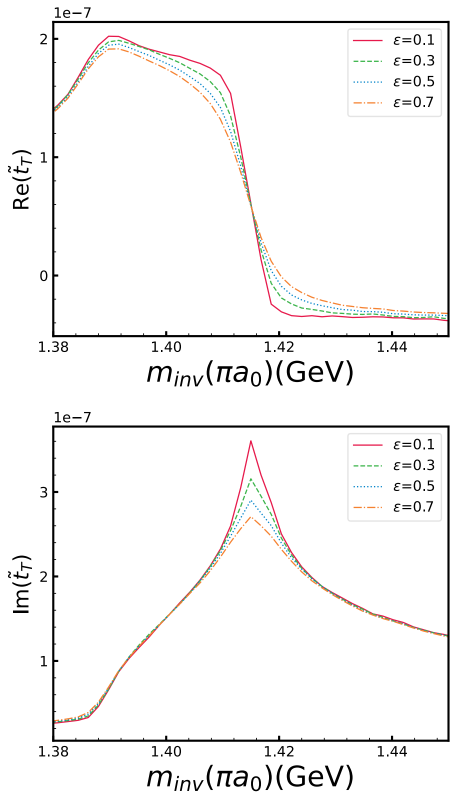

Fig. 5. (color online) The dependence of the triangle amplitude Re($\tilde{t}_T$) and Im($\tilde{t}_T$) on the widths of the internal particles is shown in the upper and lower panels, respectively. We set $m_{a_0} = 990$ MeV, which is slightly larger than the K^-K^+ threshold, and use $\Gamma_{\bar{K}^{*0}}/2 = \epsilon = 0.1$, 0.3, 0.5, and 0.7 MeV.

V. RESULTS

In Fig. 3, we first present the triangle amplitudes $\tilde{t}_T$, Im($\tilde{t}_T$), Re($\tilde{t}_T$), and $|\tilde{t}_T|^2\times 10^7$ as functions of the invariant mass $m_{\rm inv}(\pi a_0)$, with the $a_0(980)$ mass fixed at $m_{a_0} = 980$ MeV. The results for $|\tilde{t}_T|^2$ exhibit a clear peak around 1420 MeV, consistent with the condition in Eq. (1). The peaks of Im($\tilde{t}_T$) and Re($\tilde{t}_T$) appear at 1440 MeV and 1390 MeV, respectively, arising from the TS and the $\bar{K}^{*0}K^+$ threshold. From top to bottom, the results correspond to the cutoff parameters $q_{\max} = 600$, 800 and 1000 MeV, respectively. As $q_{\max}$ increases, the peak positions in Im($\tilde{t}_T$), Re($\tilde{t}_T$), and $|\tilde{t}_T|^2$ remain unchanged, while their magnitudes generally increase. The triangle amplitudes for different masses of $a_0(980)$ are shown in Fig. 4. The results indicate that the peaks remain near 1420 MeV, while the strength of the triangle amplitude increases as m_{a_0} increases. Next, we examine the behavior of the triangle amplitudes Im($\tilde{t}_T$) and Re($\tilde{t}_T$) as functions of the internal particle width.

Following Ref. [53], Fig. 5 illustrates the development of the TS by fixing $\Gamma_{K^*}/2 = \epsilon$ at different finite values close to zero. The formation of the TS in the $\bar{K}^{*0}$-K-K

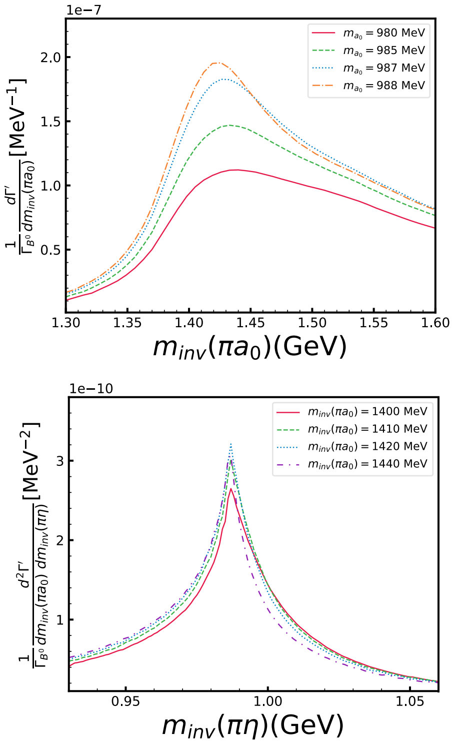

Fig. 6. (color online) The upper and lower panels show, respectively, the differential distribution $\dfrac{\mathrm{d}\Gamma'}{\mathrm{d}m_{\mathrm{inv}(\pi a_0)}}$ (Eq. 24) as a function of the invariant mass $m_{\mathrm{inv}}(\pi a_0)$ and the double differential distribution $\dfrac{1}{\Gamma_{B^0}}\dfrac{\mathrm{d}^2\Gamma'}{\mathrm{d}m_{\mathrm{inv}}(\pi a_0)\mathrm{d}m_{\mathrm{inv}}(\pi\eta)}$ (Eq. 36) as a function of the invariant masses $m_{\mathrm{inv}}(\pi a_0)$ and $m_{\mathrm{inv}}(\pi\eta)$.

triangle loop requires the $a_0(980)$ mass to be slightly above the K^-K^+ threshold; therefore, we take $m_{a_0} = 990$ MeV. The distinct origins of the peaks in $\mathrm{Re}(\tilde{t}_T)$ and $\mathrm{Im}(\tilde{t}_T)$ indicate that these two components exhibit different behaviors, as shown in the upper and lower panels of Fig. 5. Specifically, $\mathrm{Re}(\tilde{t}_T)$ exhibits a cusp at the $\bar{K}^{*0}K$ threshold around 1390 MeV, followed by a sharp decrease near the TS at 1420 MeV. In contrast, $\mathrm{Im}(\tilde{t}_T)$ develops a narrow peak at 1420 MeV, directly reflecting the emergence of the triangle singularity. Fig. 5 also shows that, as ϵ decreases, the decrease in $\mathrm{Re}(\tilde{t}_T)$ near 1420 MeV becomes steeper, the cusp near 1390 MeV becomes more pronounced, and the peak in $\mathrm{Im}(\tilde{t}_T)$ becomes increasingly sharp. In the limit $\Gamma_{K^*}/2 = \epsilon = 0$, the peak of $\mathrm{Im}(\tilde{t}_T)$ develops into a genuine singularity.

In Fig. 6, the differential distributions $\dfrac{\mathrm{d}\Gamma'}{\mathrm{d}m_{\mathrm{inv}(\pi a_0)}}$, Eq. (24), and $\dfrac{1}{\Gamma_{B^0}}\dfrac{\mathrm{d}^2\Gamma'}{\mathrm{d}m_{\mathrm{inv}}(\pi a_0)\mathrm{d}m_{\mathrm{inv}}(\pi\eta)}$, Eq. (36), are shown as functions of the invariant masses $m_{\mathrm{inv}}(\pi a_0)$ and $m_{\mathrm{inv}}(\pi\eta)$ in the upper and lower panels, respectively. In the upper panel of Fig. 6, the differential mass distribution for the $B^0 \to D^-\pi^+a_0(980)$ decay with respect to $m_{\mathrm{inv}}(\pi a_0)$ is

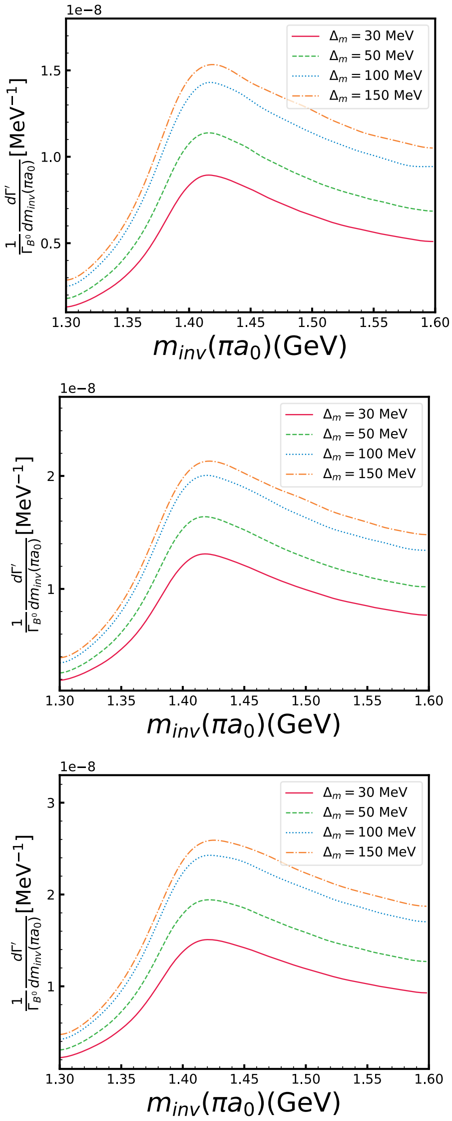

Fig. 7. (color online) The differential decay width $\dfrac{1}{\Gamma_{B^0}}\dfrac{\mathrm{d}^2\Gamma'}{\mathrm{d}m_{\mathrm{inv}}(\pi a_0)\mathrm{d}m_{\mathrm{inv}}(\pi\eta)}$ is shown as a function of the invariant mass $m_{\mathrm{inv}}(\pi a_0)$, integrated over $m_{\mathrm{inv}}(\pi\eta) \in [980\,\mathrm{MeV} - \Delta_m, 980\,\mathrm{MeV} + \Delta_m]$. From top to bottom, the curves correspond to $q_{\max} = 600, 800$ and 1000 MeV, respectively.

shown for fixed values $m_{\mathrm{inv}}(\pi\eta) = 980, 985, 987$ and 988 MeV with $q_{\max} = 600$ MeV. It is evident that increasing m_{a_0} enhances the decay width of B^0, while the peak position remains at the TS, $m_{\mathrm{inv}}(\pi a_0) \simeq 1420$ MeV. In the lower panel of Fig. 6, the dependence of $\dfrac{1}{\Gamma_{B^0}}\dfrac{\mathrm{d}^2\Gamma'}{\mathrm{d}m_{\mathrm{inv}}(\pi a_0)\mathrm{d}m_{\mathrm{inv}}(\pi\eta)}$ on $m_{\mathrm{inv}}(\pi\eta)$ is shown for fixed values $m_{\mathrm{inv}}(\pi a_0) = 1400, 1410, 1420$ and 1440 MeV around the TS. A pronounced peak appears around 980 MeV, indicating that the main contribution to the decay width comes from the region $m_{\mathrm{inv}}(\pi\eta) \simeq 980$ MeV. Moreover, the peak for $m_{\mathrm{inv}}(\pi a_0) = 1420$ MeV, close to the TS, is significantly sharper than those at the other values. Therefore, when focusing on the $a_0(980)$ region, we can integrate the double differential distribution $\frac{1}{\Gamma_B}\frac{d^2\Gamma'}{dm_{\rm inv}(\pi a_0)\,dm_{\rm inv}(\pi\eta)}$ over $m_{\rm inv}(\pi\eta)$ around $m_{\rm inv}(\pi\eta)=980$ MeV. In Fig. 7, we present the results obtained by integrating over $m_{\rm inv}(\pi\eta)\in[980\ {\rm MeV}-\Delta_m,\ 980\ {\rm MeV}+\Delta_m]$ with $\Delta_m=30$, 50, 100 and 150 MeV. The results show a clear peak at 1420 MeV when the $a_0(980)$ is considered a dynamically generated state, consistent with the results in Fig. 6. A comparison of the subfigures for $q_{\rm max}=600, 800$ and 1000 MeV shows that the decay width exhibits a slight enhancement as the cutoff parameter increases.

VI. SUMMARY

In this work, we investigate the triangle mechanism in the $B^0 \to D^-\pi^+ a_0(980)(\pi^0\eta)$ decay and explore the nature of $a_0(980)$ as a dynamically generated state arising from meson-meson interactions. The $\bar{K}^{*0}$-K^+-K^- triangle loop originates from the weak decay $B^0 \to D^-K^+\bar{K}^{*0}$, followed by $\bar{K}^{*0}\to\pi^+K^-$ and the subsequent rescattering of K^+K^- to form $a_0(980)$. We provide analytical expressions for the differential decay widths $\frac{d\Gamma}{dm_{\rm inv}(\pi a_0)}$ and $\frac{d^2\Gamma}{dm_{\rm inv}(\pi a_0)\,dm_{\rm inv}(\pi\eta)}$ corresponding to the three-body and four-body final states, respectively, including the $\bar{K}^{*0}$-K^+-K^- triangle loop amplitude. The triangle amplitude produces a pronounced peak near 1420 MeV in the $\pi a_0(980)$ invariant mass distribution, which can be interpreted as a TS signal. The dependence of the TS on the internal $\bar{K}^{*0}$ width is also investigated. The K^+K^- rescattering generates a pronounced peak near 980 MeV in the $\pi^0\eta$ invariant mass distribution, reflecting the formation of the $a_0(980)$. Meanwhile, the invariant mass spectrum of the $\pi^+\pi^0\eta$ system exhibits a peak around 1420 MeV, consistent with the results obtained from the three-body final state. Based on the current observations and analyses by the COMPASS Collaboration, we expect that B^0 decays can serve as a potential platform for further confirming the TS nature of the $a_1(1420)$ in future experiments.

References

[1] S. Navas *et al.* (Particle Data Group), Phys. Rev. D **110**, 030001 (2024)
[2] F. K. Guo, C. Hanhart, U. G. Meißner *et al.*, Rev. Mod. Phys. **90**, 015004 (2018) [Erratum: Rev. Mod. Phys. **94**, 029901 (2022)], arXiv: 1705.00141[hep-ph]
[3] S. L. Olsen, T. Skwarnicki, and D. Zieminska, Rev. Mod. Phys. **90**, 015003 (2018), arXiv: 1708.04012[hep-ph]
[4] N. Brambilla, S. Eidelman, C. Hanhart *et al.*, Phys. Rept. **873**, 1 (2020), arXiv: 1907.07583[hep-ex]
[5] R. Karplus, C. M. Sommerfield, and E. H. Wichmann, Phys. Rev. **111**, 1187 (1958)
[6] L. Landau, Nucl. Phys. **13**, 181 (1960)
[7] S. Coleman and R. E. Norton, Nuovo Cim. **38**, 438 (1965)
[8] H. B. Li (BESIII Collaboration), (2011), arXiv: 1108.5789[hep-ex]
[9] J. J. Wu, X. H. Liu, Q. Zhao *et al.*, Phys. Rev. Lett. **108**, 081803 (2012), arXiv: 1108.3772[hep-ph]
[10] F. Aceti, W. H. Liang, E. Oset *et al.*, Phys. Rev. D **86**, 114007 (2012), arXiv: 1209.6507[hepph]
[11] X. G. Wu, J. J. Wu, Q. Zhao *et al.*, Phys. Rev. D **87**, 014023 (2013), arXiv: 1211.2148[hep-ph]
[12] N. N. Achasov, A. A. Kozhevnikov, and G. N. Shestakov, Phys. Rev. D **92**, 036003 (2015), arXiv: 1504.02844[hepph]
[13] F. Aceti, J. Dias, and E. Oset, Eur. Phys. J. A **51**, 48 (2015), arXiv: 1501.06505[hep-ph]
[14] M. Mikhasenko, B. Ketzer, and A. Sarantsev, Phys. Rev. D **91**, 094015 (2015), arXiv: 1501.07023[hep-ph]
[15] F. K. Guo and U. G. Meissner, Phys. Rev. Lett. **108**, 112002 (2012), arXiv: 1111.1151[hep-ph]
[16] X. G. Wu and Q. Zhao, PoS **QNP2012**, 087 (2012), arXiv: 1206.4512[hep-ph]
[17] G. Li, F. l. Shao, C. W. Zhao *et al.*, Phys. Rev. D **87**, 034020 (2013), arXiv: 1212.3784[hep-ph]
[18] X. H. Liu, PoS **Hadron2013**, 041 (2013)
[19] Q. Wang, C. Hanhart, and Q. Zhao, Phys. Rev. Lett. **111**, 132003 (2013), arXiv: 1303.6355[hep-ph]
[20] Q. Wang, C. Hanhart, and Q. Zhao, Phys. Lett. B **725**, 106 (2013), arXiv: 1305.1997[hep-ph]
[21] X. H. Liu and G. Li, Phys. Rev. D **88**, 014013 (2013), arXiv: 1306.1384[hep-ph]
[22] X. G. Wu, C. Hanhart, Q. Wang *et al.*, Phys. Rev. D **89**, 054038 (2014), arXiv: 1312.5621[hep-ph]
[23] X. H. Liu, Phys. Rev. D **90**, 074004 (2014), arXiv: 1403.2818[hep-ph]
[24] M. Bayar, F. Aceti, F. K. Guo *et al.*, Phys. Rev. D **94**, 074039 (2016), arXiv: 1609.04133[hep-ph]
[25] N. N. Achasov, A. A. Kozhevnikov, and G. N. Shestakov, Phys. Rev. D **93**, 114027 (2016), arXiv: 1604.00177[hepph]
[26] R. Pavao, S. Sakai, and E. Oset, Eur. Phys. J. C **77**, 599 (2017), arXiv: 1706.08723[hep-ph]
[27] F. Aceti, L. R. Dai, and E. Oset, Phys. Rev. D **94**, 096015 (2016), arXiv: 1606.06893[hep-ph]
[28] S. Sakai, E. Oset, and W. H. Liang, Phys. Rev. D **96**, 074025 (2017), arXiv: 1707.02236[hep-ph]
[29] W. H. Liang, S. Sakai, J. J. Xie *et al.*, Chin. Phys. C **42**, 044101 (2018), arXiv: 1711.04603[hep-ph]
[30] N. N. Achasov and G. N. Shestakov, JETP Lett. **107**, 276 (2018) [Pisma Zh. Eksp. Teor. Fiz. **107**(5), 292 (2018)], arXiv: 1804.10749[hep-ph]
[31] J. Lu, X. Luo, M. Song *et al.*, Chin. Phys. C **47**, 073103 (2023), arXiv: 2212.13008[hep-ph]
[32] F. K. Guo, X. H. Liu, and S. Sakai, Prog. Part. Nucl. Phys. **112**, 103757 (2020), arXiv: 1912.07030[hep-ph]
[33] H. J. Jing, S. Sakai, F. K. Guo *et al.*, Phys. Rev. D **100**, 114010 (2019), arXiv: 1907.12719[hep-ph]
[34] W. H. Liang, H. X. Chen, E. Oset *et al.*, Eur. Phys. J. C **79**, 411 (2019), arXiv: 1903.01252[hep-ph]
[35] Q. Huang and J. J. Wu, (2021), arXiv: 2109.08349[hepph]
[36] Q. Huang, Z. X. Ma, J. J. Wu *et al.*, Phys. Rev. D **110**, 034018 (2024), arXiv: 2405.11127[hep-ph]
[37] C. W. Xiao, J. M. Dias, L. R. Dai *et al.*, Phys. Rev. D **109**, 074033 (2024), arXiv: 2402.17584[hep-ph]
[38] H. P. Li, W. H. Liang, C. W. Xiao *et al.*, (2025), arXiv: 2512.11681[hep-ph]

[39] K. Wang, R. Li, and B. C. Liu, Phys. Rev. D **108**, 094027 (2023), arXiv: 2307.03372[hep-ph]
[40] S. Sakai, Phys. Rev. D **101**, 074041 (2020), arXiv: 2002.08594[hep-ph]
[41] J. J. Xie and F. K. Guo, Phys. Lett. B **774**, 108 (2017), arXiv: 1709.01416[hep-ph]
[42] L. R. Dai, R. Pavao, S. Sakai *et al*., Phys. Rev. D **97**, 116004 (2018), arXiv: 1804.01136[hep-ph]
[43] Y. Y. Li, J. Song, E. Oset *et al*., Eur. Phys. J. C **85**, 1086 (2025), arXiv: 2505.21403[hep-ph]
[44] S. C. Zhang, M. Y. Duan, W. T. Lyu *et al*., Eur. Phys. J. C **84**, 1253 (2024), arXiv: 2405.14235[hep-ph]
[45] K. Wang, Y. F. Wang, B. C. Liu *et al*., Phys. Rev. D **110**, 094017 (2024), arXiv: 2408.12965[hep-ph]
[46] J. J. Xie and E. Oset, Phys. Lett. B **792**, 450 (2019), arXiv: 1811.07247[hep-ph]
[47] X. Z. Ling, M. Z. Liu, J. X. Lu *et al*., Phys. Rev. D **103**, 116016 (2021), arXiv: 2102.05349[hep-ph]
[48] Y. K. Hsiao, Y. Yu, and B. C. Ke, Eur. Phys. J. C **80**, 895 (2020), arXiv: 1909.07327[hep-ph]
[49] M. Bayar, R. Molina, E. Oset *et al*., Phys. Rev. D **109**, 076027 (2024), arXiv: 2312.12004[hep-ph]
[50] Z. M. Ding, H. Y. Jiang, and J. He, Eur. Phys. J. C **80**, 1179 (2020), arXiv: 2011.04980[hep-ph]
[51] S. Sakai, E. Oset, and F. K. Guo, Phys. Rev. D **101**, 054030 (2020), arXiv: 2002.03160[hep-ph]
[52] R. Molina and E. Oset, Eur. Phys. J. C **80**, 451 (2020), arXiv: 2002.12821[hep-ph]
[53] S. Sakai, E. Oset, and A. Ramos, Eur. Phys. J. A **54**, 10 (2018), arXiv: 1705.03694[hep-ph]
[54] Y. H. Ge, X. H. Liu, and H. W. Ke, Eur. Phys. J. C **81**, 854 (2021), arXiv: 2103.05282[hep-ph]
[55] X. L. Ren, K. P. Khemchandani, and A. Martinez Torres, Phys. Rev. D **102**, 016005 (2020), arXiv: 1912.03369[hep-ph]
[56] Y. H. Ge, X. H. Liu, and H. W. Ke, Eur. Phys. J. C **82**, 955 (2022), arXiv: 2207.09900[hep-ph]
[57] S. X. Nakamura, Phys. Rev. D **100**, 011504 (2019), arXiv: 1903.08098[hep-ph]
[58] S. X. Nakamura, Phys. Rev. D **102**, 074004 (2020), arXiv: 1912.11830[hep-ph]
[59] D. Samart, W. h. Liang, and E. Oset, Phys. Rev. C **96**, 035202 (2017), arXiv: 1703.09872[hep-ph]
[60] L. R. Dai, Q. X. Yu, and E. Oset, Phys. Rev. D **99**, 016021 (2019), arXiv: 1809.11007[hep-ph]
[61] E. Oset and L. Roca, Phys. Lett. B **782**, 332 (2018), arXiv: 1803.07807[hep-ph]
[62] L. R. Dai, L. Roca, and E. Oset, Phys. Rev. D **99**, 096003 (2019), arXiv: 1811.06875[hep-ph]
[63] E. Wang, J. J. Xie, W. H. Liang *et al*., Phys. Rev. C **95**, 015205 (2017), arXiv: 1610.07117[hepph]
[64] V. R. Debastiani, S. Sakai, and E. Oset, Phys. Rev. C **96**, 02520 (2017), arXiv: 1703.01254[hep-ph]
[65] X. Y. Wang, L. L. Wang, X. H. Liu *et al*., (2025), arXiv: 2510.23099[hep-ph]
[66] X. Wei, Q. H. Shen, X. H. Liu *et al*., Phys. Rev. D **113**, 014022 (2026), arXiv: 2509.12552[hep-ph]
[67] M. Bayar, R. Pavao, S. Sakai *et al*., Phys. Rev. C **97**, 035203 (2018), arXiv: 1710.03964[hep-ph]
[68] N. Ikeno, R. Molina, and E. Oset, Phys. Rev. C **104**, 014614 (2021), arXiv: 2103.01712[nucl-th]
[69] Y. Gao, Y. Jia, Y. Lin *et al*., Mod. Phys. Lett. A **39**, 2450141 (2024), arXiv: 2211.12920[hep-ph]
[70] J. J. Xie, L. S. Geng, and E. Oset, Phys. Rev. D **95**, 034004 (2017), arXiv: 1610.09592[hep-ph]
[71] Y. Huang, M. Z. Liu, J. X. Lu *et al*., Phys. Rev. D **98**, 076012 (2018), arXiv: 1807.06485[hepph]
[72] L. Roca and E. Oset, Phys. Rev. C **95**, 065211 (2017), arXiv: 1702.07220[hep-ph]
[73] X. H. Liu, G. Li, J. J. Xie *et al*., Phys. Rev. D **100**, 054006 (2019), arXiv: 1906.07942[hep-ph]
[74] J. J. Xie, G. Li, and X. H. Liu, Chin. Phys. C **44**, 114104 (2020), arXiv: 1907.12202[hep-ph]
[75] V. R. Debastiani, S. Sakai, and E. Oset, Eur. Phys. J. C **79**, 69 (2019), arXiv: 1809.06890[hep-ph]
[76] Y. Huang, J. X. Lu, J. J. Xie *et al*., Eur. Phys. J. C **80**, 973 (2020), arXiv: 2008.07959[hep-ph]
[77] Y. Huang, C. j. Xiao, Q. F. Lü *et al*., Phys. Rev. D **97**, 094013 (2018), arXiv: 1801.03598[hep-ph]
[78] X. H. Liu, M. Oka, and Q. Zhao, Phys. Lett. B **753**, 297 (2016), arXiv: 1507.01674[hep-ph]
[79] Q. Li, C. H. Chang, X. Tong *et al*., JHEP **10**, 098 (2025), arXiv: 2503.08440[hepph]
[80] N. N. Achasov and G. N. Shestakov, Phys. Rev. D **110**, 016023 (2024), arXiv: 2405.09228[hep-ph]
[81] C. W. Shen, H. J. Jing, F. K. Guo *et al*., Symmetry **12**, 1611 (2020), arXiv: 2008.09082[hep-ph]
[82] C. Adolph *et al*. (COMPASS Collaboration), Phys. Rev. Lett. **115**, 082001 (2015), arXiv: 1501.05732[hep-ex]
[83] G. D. Alexeev *et al*. (COMPASS Collaboration), Phys. Rev. Lett. **127**, 082501 (2021), arXiv: 2006.05342[hep-ph]
[84] R. Molina, M. Doering, W. H. Liang *et al*., Eur. Phys. J. C **81**, 782 (2021), arXiv: 2107.07439[hep-ph]
[85] I. Adachi *et al*. (Belle-II Collaboration), JHEP **08**, 206 (2024), arXiv: 2406.06277[hep-ex]
[86] W. H. Liang and E. Oset, Phys. Lett. B **737**, 70 (2014), arXiv: 1406.7228[hep-ph]
[87] J. A. Oller and E. Oset, Nucl. Phys. A **620**, 438 (1997) [Erratum: Nucl. Phys. A **652**, 407 (1999)], arXiv: hep-ph/9702314
[88] J. A. Oller, E. Oset, and J. R. Pelaez, Phys. Rev. D **59**, 074001 (1999) [Erratum: Phys. Rev. D **60**, 099906 (1999), Erratum: Phys. Rev. D **75**, 099903 (2007)], arXiv: hep-ph/9804209
[89] S. Scherer, Adv. Nucl. Phys. **27**, 277 (2003), arXiv: hepph/0210398
[90] A. Pich, Rept. Prog. Phys. **58**, 563 (1995), arXiv: hepph/9502366
[91] J. J. Xie, L. R. Dai, and E. Oset, Phys. Lett. B **742**, 363 (2015), arXiv: 1409.0401[hep-ph]